Int. J. Electrochem. Sci., 15 **(2020)** 12504 – 12523, doi: 10.20964/2020.12.80

International Journal of
ELECTROCHEMICAL
SCIENCE
www.electrochemsci.org

Five-axis Numerical Control of Electrochemical Mechanical Polishing of an Integral Impeller

Bo Xu[1,2,*], *Weimin Gan*[1,2], *Yafeng He*[1,2], *Xiangzhi Wang*[1,2], *Feihong Yin*[1], , *Xin Wang*[2]

[1] School of Aeronautics and Mechanical Engineering, Changzhou institute of Technology, Changzhou 213002, P.R. China
[2] Key Laboratory of Special Procegesand of Colleges and University of Jiangsu Province, Changzhou 213002, P.R. China
[3] School of Mechanical Engineering, Changzhou University, Changzhou 213164, P.R. China
[*]E-mail: xubo125@163.com

Received: 30 July 2020 / *Accepted:* 19 September 2020 / *Published:* 31 October 2020

The blade surface morphology has a significant impact on the life, performance, and stability of aero-engine integral impellers. The surface roughness of such free-form surfaces can be reduced using numerical control electrochemical mechanical polishing (NC ECMP), which is a combination of CNC technology, electrolytic polishing, and mechanical grinding. In this study, based on a YG8 cemented carbide specimen, two types of cathode polishing plate materials were compared and selected. The electrolyte ratio was optimized by conducting an orthogonal test. The relationship between the voltage, feed speed, spindle speed, duty cycle, cathode positive pressure, and surface roughness were studied. Finally, an integral impeller was polished under a set of optimized parameters, and its surface roughness was reduced from Ra 0.85 μm to Ra 0.215 μm. Our results confirm that the five-axis NC ECMP is an economical and effective method for polishing complex surfaces, particularly in aerospace applications.

Keywords: Integral Impeller; Cemented Carbide; NC Electrochemical Mechanical Polishing; Surface Morphology

1. INTRODUCTION

An integral impeller is the key part of aero-engines. The quality, performance, and stability of such products can be improved by optimizing the surface roughness and manufacturing accuracy. Through comparative experiments, Zidane analyzed the influence of blade surface roughness on engine aerodynamics and established a relationship between the surface roughness and the Reynolds coefficient. The difference in the energy consumptions between high- and low-roughness surfaces was found to be 40% [1]. Luis studied the influence of blade roughness on the performance of a vertical-axis tidal turbine through experimental research. After testing three different blade surface roughness values, Luis found that the turbine performance decreased significantly when operated under a high Reynolds number and high-roughness blade [2]. By reviewing studies conducted over the past 60 years, Bons summarized the influence of surface roughness on the turbine performance, and pointed out that a multi-scale modeling is required to predict the surface heat flow and pressure distribution [3]. NASA studied the flow distribution law and roughness effect of turbine blade passages, and realized the control of separation flow to enhance the performance of products. Rolls Royce (UK) demonstrated that the roughness of a turbine blade can be reduced from Ra 0.5 μm to Ra 0.2 μm by increasing its manufacturing accuracy from 60 μm to 12 μm. This corresponded to an increase in the compression efficiency of the engine from 87% to 93%. Even when the machining accuracy could not meet this requirement, the compression efficiency could still be increased by 3% by reducing the blade surface roughness from Ra 3.2 μm to Ra 0.6 μm. When the roughness was reduced to 10% of the current value, the thermal efficiency of the engine could be doubled [4-7].

Polishing methods for integral impellers include manual polishing; the roughness of a blade after manual polishing is generally between Ra 1.5 μm and Ra 0.7 μm. However, this method is time-consuming and laborious, it is difficult to ensure the shape and dimensional accuracy of the products, and the processing quality is uncontrollable. Another method is abrasive belt polishing, which is a type of elastic grinding technique that can be used to simultaneously perform grinding and polishing, suitable for polishing blade surfaces. By conducting various polishing tests on titanium alloy parts of aero-engines, D.A. Axinte (UK) confirmed the feasibility of abrasive belt grinding for finishing complex curved surfaces, and optimized the processing parameters by conducting multiple tests [8]. Metabo, a German company, developed special precision polishing machine tools for turbine blades and steam turbine blades, which are widely introduced in developed countries. The six-axis CNC blade belt grinding machine developed by Ex-Cell-O (United States) can be used to grind two cylindrical blades simultaneously. The maximum size of the blade is 1500 mm × 330 mm, and the working time required is only 3.5 h [9]. With the popularization and application of robot systems, the efficiency of abrasive belt polishing of blades has been further improved. Huang developed an intelligent grinding and polishing system for engine turbine blades. The tests conducted showed that the efficiency of blade surfaces processed by this system was approximately 40% higher than that processed by conventional manual polishing while ensuring surface quality and precision [10]. Another polishing method is abrasive flow polishing. To overcome fracture failures that often occur in the operation of aerospace engine integral impellers, Dynetics (United States) adopted an abrasive flow processing method to process the blade profile and effectively reduced the cracks and residual stress generated in the previous processing [11]. Scanning electron microscopy can be used to observe abrasive flow-machined surfaces. Williams compared different methods of initial machining surface and abrasive flow machining, and concluded that the original surface of a workpiece and the concentration of the abrasive particles were vital to the machining quality. A high surface accuracy could be obtained through cyclic machining, and abrasive flow polishing had a significant effect on improving the surface after applying EDM [12]. Fadaie introduced electrolytic polishing in the 1990s, where a pulse power was used instead of a DC power supply to carry out electrochemical mechanical composite machining. The research showed that the proportions of electrolytic and mechanical removal could be adjusted by adjusting the pulse width and pulse width combinations, for a more convenient control of the machining process and optimization of the process parameters [13]. Kozak carried out several tests on the curved surface machining of simple spherical cathodes. By establishing the corresponding mathematical model and process tests, Kozak explored the influences of processing voltage, machining gap, tool radius, and tool feed speed on the electrolytic etching amount and surface roughness of a sample surface [14]. Sun designed a pulse electrochemical finishing technology combined with positive and negative electric fields to solve the polishing problem of titanium alloys and other difficult-to-machine mold materials. The author improved the micromorphology of the mold surface and reduced the surface roughness to a certain extent [15]. Lee applied the electrochemical mechanical polishing (ECPM) method for stainless steel substrates of thin film solar cells. With an ECMP system, the influences of electrolyte composition, voltage, polishing time, and other parameters on the polishing quality were analyzed. The optimized results achieved a mirror effect on SS304 polishing [16].

The performance of aerospace engines can be further improved by reducing the runaway loss of the body impeller and improving the overall surface quality. The existing blade surface polishing technologies are only suitable for general performance requirements. In this study, through an experimental analysis of numerical control electrochemical mechanical polishing (NC ECMP), a new process method is established for the surface finishing of integral impeller blades.

2. PRINCIPLES OF NC ELECTROCHEMICAL MECHANICAL POLISHING

The NC ECMP is a new technology based on the electrochemical finishing technology, which still follows Faraday’s law. It combines the advantages of NC machining, electrochemical machining, and mechanical grinding, and can be used to effectively polish complex surfaces and difficult-to-machine materials. Figure 1(a) shows that the five-axis CNC ECMP machine can move in the X, Y, and Z axes, swing along the b axis, and rotate about the C axis; thus, it can process free-form surfaces. Figure 1(b) shows the structure of the cathode. The main part of the cathode is a cylinder, the side wall is provided with an insulating coating, the polishing edge is a hemispherical body with an exposed bottom end, and a polishing plate is arranged at the middle of the hemispherical body. Because the polishing plate is located at the top of the cathode ball head, the angle between the cathode axis and the normal surface of the workpiece should be controlled during the polishing process to make the exposed cathode head face the polished surface, so as to improve the polishing efficiency. The cathode is clamped on the spindle (Z axis) through the tool handle and connected to the negative pole of the power supply. The impeller is installed on the workbench in the C axis. The electrolyte is extracted from the electrolyte box using a working pump, and is sprayed onto the processing area through multiple external nozzles or internal nozzles evenly distributed around the cathode. During the polishing, the cathode rotates with the spindle, and an NC program is executed along the polishing track, as shown in state 1 in Fig. 1(b). When the working edge of the exposed cathode is in direct contact with the blade, the part closest to the cathode is subjected to electrochemical polishing under the combined action of the electric field and electrolyte. The workpiece surface is dissolved as it undergoes an electrochemical reaction, and a dense passive film is formed, which hinders the further reaction of the polishing, such as in region 1. During the polishing, because of the small distance between the convex part and the cathode, the metal microsurface is first quickly dissolved by the electrochemical reaction under the electric field cusp efficiency. The thickness d1 of the metal oxide or hydroxide generated by the microsurface is greater than that of the low-lying area, i.e., the convex part is removed to a greater extent than the low-lying part. When the cathode is rotated by 90° to state 2 of the mechanical polishing state, the passivation film on the workpiece surface is mechanically polished by the polishing plate at the end of the cathode, so that the metal matrix of the convex part is exposed, and the passive film in the low-lying area is retained because the polishing plate cannot grind it. When the cathode is rotated by 90° to state 1, the bare metal substrate at the bulge is polished again to produce a passive film. Because of the existence of the original passive film in the low-lying area, there is less passive film formation, i.e., the metal bodies in the low-lying area participate in the reaction. The cathode is rotated by 90° to remove the passivation film on the workpiece surface again to prepare for the next state. The cathode is rotated by 180° to complete the electrochemical polishing and mechanical polishing. The material at the convex and low-lying parts of the workpiece surface is polished and removed. However, the amount of material removed from the convex part is greater than that removed from the low-lying part, and the relative height difference between the convex and low-lying parts is gradually reduced, i.e., the roughness value of the workpiece surface is reduced, thus improving the surface quality of the workpiece.

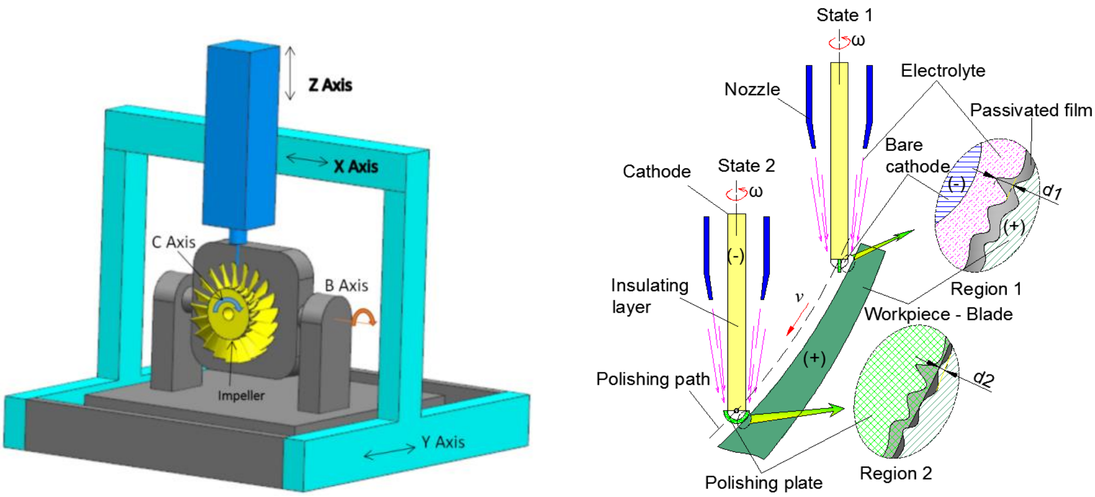

Figure 1. (a) CNC electrochemical mechanical polishing (ECMP) machine, and (b) Mechanism of CNC ECMP

To analyze the final morphology and surface quality of the blade surface processed using the NC ECMP, the machining conditions are set as follows: the initial surface expression of the workpiece is $z = Z_0 (x, y)$; the cathode tool is a ball head with radius R (excluding the grinding and polishing pieces); the initial position of the cathode tool in the workpiece coordinate system is (x_e (0), y_e (0), z_e (0)); the coordinate for the moving path of the cathode tool is (x_e (t), y_e (t), z_e (t)); the processing voltage is U; the conductivity is κ; the amount of electrolytic removal of the workpiece K*v* = K*v*(*i*) (*i* is the current density). The position of the cathode tool is represented in the workpiece coordinate system, and the workpiece surface at any time can be described using the equation z = Z (x, y, t). The surface shape equation for the workpiece can be expressed as follows:

$$\frac{\partial Z}{\partial t} = Kv(i_A)i_A\sqrt{1+\left(\frac{\partial Z}{\partial X}\right)^2+\left(\frac{\partial Z}{\partial y}\right)^2} \quad (1)$$

The initial processing conditions are t = 0 and z = Z_0 (x, y) (initial surface equation for the workpiece).

The current density i_A on the workpiece surface can be approximately calculated from the linear potential distribution at the fixed points of the anode and cathode [17]. Assuming that the conductivity remains constant, we can express i_A as:

$$i_A = k_0\frac{U-E(i_A)}{d} \quad (2)$$

For NC ECMP with a composite cathode, the machining gap *d* is expressed as follows:

$$d=\sqrt{(x-x_e)^2+(y-y_e)^2+(z-z_e)^2}-R \quad (3)$$

The point (x_e, y_e, z_e) is the spherical center coordinate of the spherical head composite cathode tool, and its motion equation is x = x_e (t), y = y_e (t), and z = z_e (t). Because the removed thickness d_e of the polishing workpiece is far less than the machining gap *d*, we have d ≈ D-R [18], where D represents the radius of the composite cathode ball head containing the mechanical grinding layer.

In terms of compound polishing and considering the above conditions, it can be seen that:

(1) The polishing voltage U determines the current density i_A, which in turn determines the material removal. Appropriately setting the voltage is an important factor in ECMP. Under the condition of micro removal and thin passive film formation, the processing voltage should be as low as possible.

(2) The tool radius R determines the machining clearance d and thus indirectly affects i_A. When designing a composite cathode, its radius r should be strictly controlled. However, the thickness of the spherical surface should be less than 2 mm under the minimum radius condition of the ball.

(3) The processing time directly affects the processing effect. In a certain range, the depth of the surface finishing increases with the increase in the processing time, and the surface becomes smooth gradually.

3. SYSTEM SETUP AND EXPERIMENTAL

3.1. Five-axis CNC electrochemical mechanical polishing machine

Figure 2 shows a five-axis CNC electrochemical mechanical compound machining tool. It is based on a five-axis CNC machine tool, which is modified by adding a composite cathode, a special tool handle, a marble table, an electrolyte filter, a supply device, a processing power supply, and a protection device.

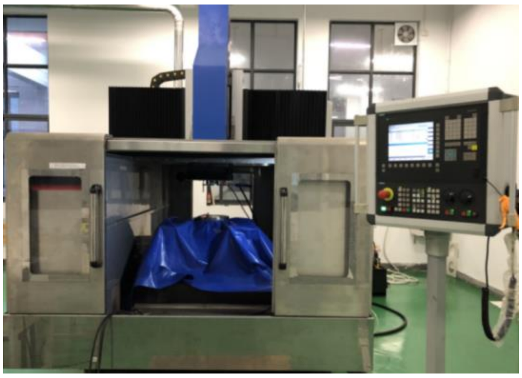

Figure 2. Five-axis CNC electrochemical mechanical polishing machine

3.2. Design of cathode

Figure 3 shows the structure of the cathode. The cathode rod is made of SUS304 stainless steel, and the side wall has an insulating layer to prevent stray corrosion. The polishing edge of the cathode is a hemispherical body, and the ball head has a grinding plate and a bolt at the middle. There are four liquid channels around the ball head, to spray the electrolyte from the internal flow channel of the cathode to the processing area.

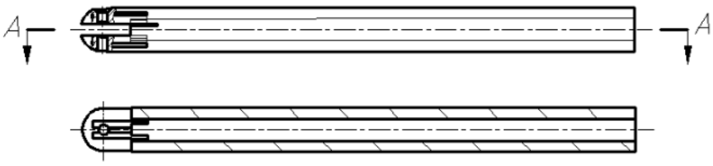

Figure 3. Cathode structure design

3.3. Preparation for foundation test

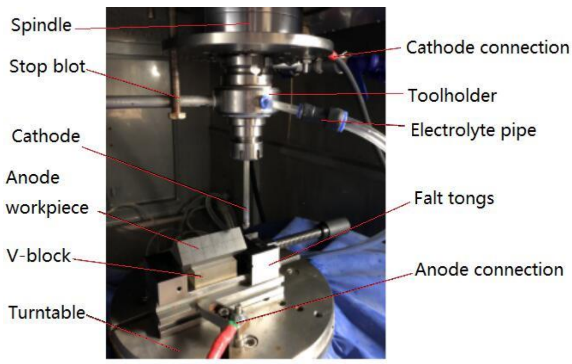

Figure 4. NC ECMP device for basic test

To determine the suitable polishing parameters for the cathode of the polyurethane polishing wafer and YG8 cemented carbide workpiece, and simulate the polishing of the blade surface, the workpiece was installed at an angle of 45°. The initial surface roughness of the YG8 cemented carbide square bar with a workpiece size of 30 mm × 30 mm × 90 mm is approximately Ra 1.85 μm. Figure 4 shows the basic test device of the NC ECMP.

4. RESULTS AND DISCUSSION

4.1. Material selection of cathode polishing plate

The material of the mechanical abrasive is an important parameter in ECMP, as it directly determines the surface quality of the workpiece. Abrasives come with different properties. The commonly used abrasives are brown corundum, white corundum, and black silicon carbide. In this study, CBN and polyurethane polishing wafer are selected for a comparative research.

The composite cathode abrasive material shown in Fig. 5 is CBN, which is a type of superhard material whose hardness is second only to that of diamond.

Figure 5. Cathode with a CBN abrasive plate

Figure 6 shows a polyurethane polishing pad composite cathode, which is made of a polyurethane foam with micropores as the matrix and solid abrasive particles. By adjusting the raw materials and formula, the polishing materials with hard, semi-hard, or soft series can be made, with advantages such as wide application, environmental protection, long service life, and stable processing quality.

Figure 6. Cathode with a polyurethane polishing plate

To compare the two composite cathodes in terms of their advantages and disadvantages, a polishing contrast experiment was carried out twice. Figure 7 shows the comparative test results under different voltages. Clearly, the surface roughness of the workpiece processed by the polyurethane polishing chip is lower than that of the CBN abrasive. The results show that the composite machining phenomenon is evident when the polyurethane polishing sheet is used in the composite cathode processing, and the surface quality of the workpiece is improved by the electrolytic action and mechanical action of the polishing plate. When the CBN abrasive compound cathode polishing is used, the mechanical action is stronger than the electrolytic effect, resulting in a bright processing area and evident mechanical scratches. Moreover, the process setting the tool for the CBN abrasive composite cathode is more complex, the tool setting is shallow, and the polishing effect is not evident. If the tool setting is deeper, more heat will be generated, which will lead to overheating and scorching in the processing area. At this time, although the surface roughness of the workpiece is improved, the abrasive wear is aggravated, which can even damage the cathode. In contrast, the slightly elastic polyurethane polishing sheet can be more easily handled in the tool setting process. Through the measurement of the residual stress on the workpiece surface, it is found that the mechanical force in the CBN composite cathode polishing process is high, and the original residual stress of the workpiece is changed. In comparison, owing to the soft polyurethane material, the residual stress on the workpiece surface is largely unchanged. Kulyk et al. studied the influence of soft and hard polymer pads on the morphology of a planarized copper surface. They found that the dishing effect could be eliminated using the hard polyurethane pad [19,20]. Jeong et al. reported a high MRR in the copper ECM planarization process when using a polyurethane pad [19,21]. Based on the above analysis, a polyurethane polishing plate composite cathode was selected in the subsequent experiments.

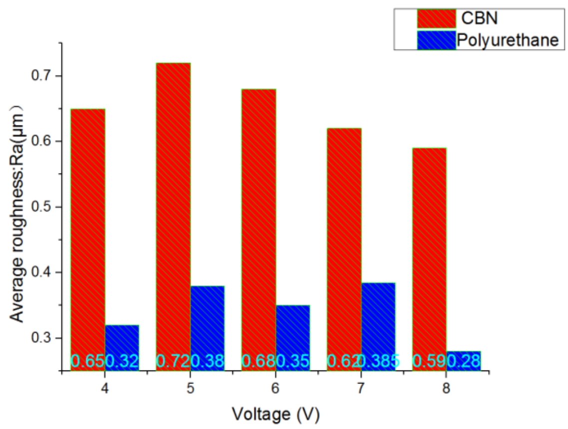

Figure 7. Comparison of surface roughness between CBN abrasive composite cathode and polyurethane polishing plate composite cathode (duty cycle: 50%, feed rate: 50 mm/min, rotational speed: 1000 rpm, polishing NC program row spacing: 0.2 mm, pressure: 0.01 kg/mm^2)

4.2 Electrolyte

The commonly used electrolytes are sodium chloride (NaCl, 5%–25%) [35], sodium nitrate ($NaNO_3$,10%–20%), sulfuric acid (H_2SO_4, 8%–20%), and sodium hydroxide (NaOH, 5%–20%) [19,22]. However, the stray corrosion is serious when sodium chloride is used in the electrolysis, and when the capacity of the electrolyte is high, sulfuric acid, which has a corrosive effect on equipment, is unsuitable for use. Aksu Serdar studied the effect of electrochemical polarization on copper removal rates during polishing with the use of EDTA slurries as the electrolyte. The experimental results demonstrated synergistic interactions between the electrochemical and mechanical forces in the copper

CMP process, indicating that an enhanced material removal and planarization could only be achieved when the electrochemical and mechanical components act together in a favorable manner [23]. Huo et al. reported that the ECP results in a low surface roughness (Ra < 10 nm) when using solutions of ethylene glycol (GE) and other acidic electrolytes [24].

In this experiment, the YG8 cemented carbide is processed, and its main components are tungsten and cobalt. Based on related literature, the composite electrolyte contains NaOH and $NaNO_3$, and a complexing agent (EDTA) and a thickener (ethylene glycol) are added. A set of experiments is carried out to explore the proportion relationship of each component. The mass fractions of each component are obtained by conducting an orthogonal test on the four components in the composite electrolyte at different mass fractions, as listed in Table 1.

Table 1. Level table of orthogonal test factors

	A $NaNO_3$/%	B NaOH/%	C EDTA/%	D EG/%
1	6	8	2	2
2	8	10	4	4
3	10	12	6	6
4	12	14	8	8
5	14	16	10	10

The processing voltage, duty cycle, cathode feed rate, rotational speed, polishing NC program row spacing, cathode positive pressure, and number of cycles were set to 6 V, 50%, 50 mm/min, 1000 rpm, 0.2 mm, 0.01 kg/mm^2, and 3, respectively. The influence of the mass fractions of each component on the surface roughness is obtained experimentally. Figure 8 shows the results. As shown in Fig. 8(a), the low concentration of sodium nitrate helps improve the surface roughness, the influence of NaOH on the surface roughness is first reduced and then increased, and the Ra reaches the optimal value when the mass fraction of the EDTA is 10%. The surface roughness decreases with the increase in the EDTA mass fraction, and the EG has a varied influence on Ra, and an increase in EG helps reduce the Ra value.

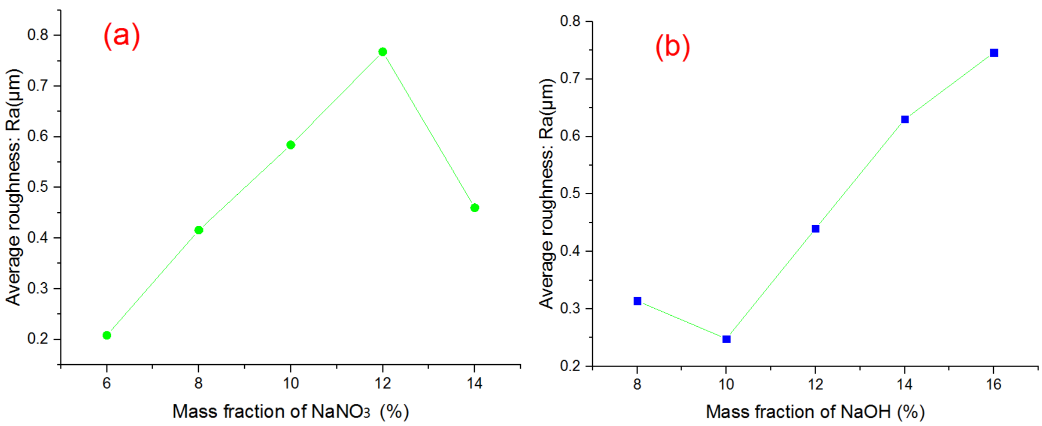

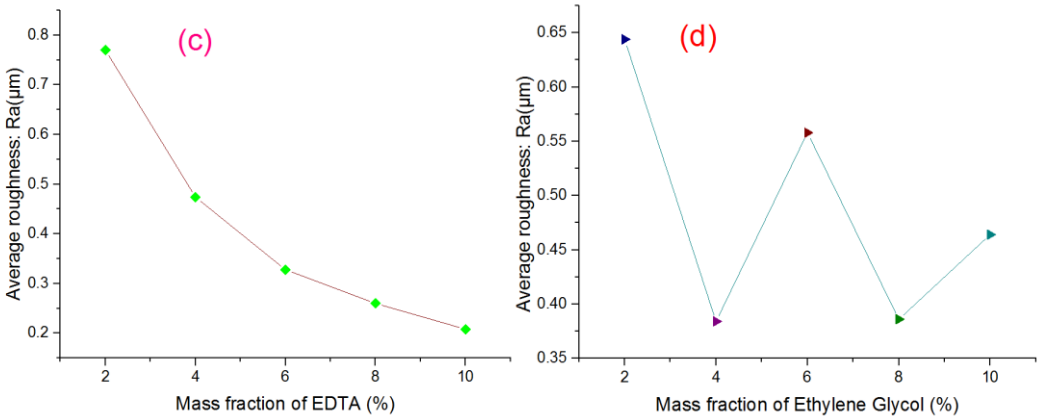

Figure 8. Fraction–Ra curves with different electrolytes: (a) $NaNO_3$, (b) NaOH, (c) EDTA, (d) EG

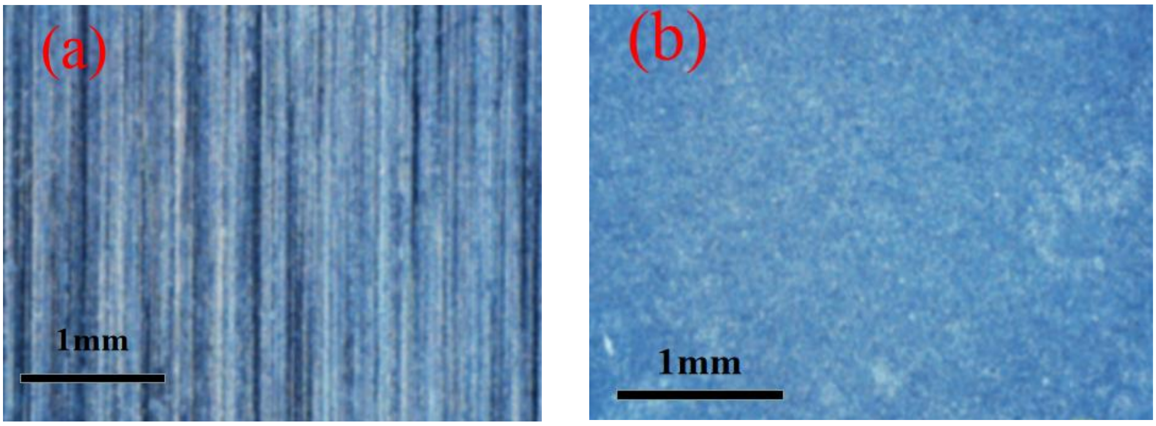

Figure 9. Microsurfaces before and after ECMP: (a) Original surface (Ra: 1.85 μm); (b) Surface after ECMP (Ra: 0.346 μm)

It can be concluded from the above table that the effects of various factors on the surface roughness of the workpiece are respectively C (EDTA), A ($NaNO_3$), B (NaOH), and D (EG), and the optimal scheme should be A1B2C5D2. The results show that the surface roughness is Ra 0.346 μm. Figure 9 shows the polishing results obtained after optimizing the original microsurface and electrolyte ratio of the workpiece.

4.3 Voltage

A suitable range of the polishing voltage can be determined by conducting process tests based on the original surface roughness and electrolyte concentration. The higher the voltage, the higher the current density and the faster the dissolution of the workpiece surface; however, the surface quality is difficult to control. The surface quality is better when low-voltage processing is adopted, though the efficiency is low; in the process of composite polishing, the current density is low, the electrochemical effect is weak, and the passive film is poor. Therefore, the surface quality of the workpiece cannot be ensured. When the duty cycle is 20%, the cathode speed is 1500 rpm, and the feed speed is 15 mm/min. Figure 10 shows the relationship between the voltage and the surface roughness.

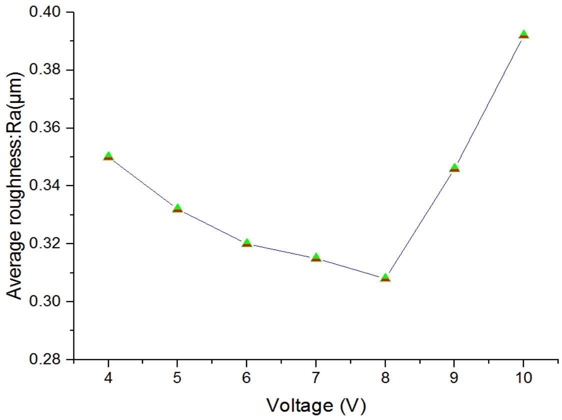

Figure 10. Influence of voltage on the average roughness

Figure 10 shows that under the same processing conditions, the surface roughness of the workpiece first decreases with the increase in the processing voltage, and when the voltage is 8 V, the surface roughness of the workpiece is minimum, and then increases gradually. When the processing voltage is too low, the electrolysis effect is weak, the current density is low, the thickness of the passive film is low, the grinding effect of the composite cathode is less, the loss is high, and the polishing effect is poor. When the voltage is too high, the current density increases, and the thickness of the passive film decreases with the increase in the voltage. If the voltage is too high, there will be no passivation film, the surface quality of the workpiece cannot be well controlled, and the stray corrosion will result in serious pitting corrosion. Figure 11 shows the microsurface after low-voltage and high-voltage polishing. Compared with the original surface shown in Fig. 9(a), due to the weak electric field strength, the surface shown in Fig. 11(a) retains the original stripe pattern, the texture distribution is fine after polishing, and the surface quality is significantly improved. In Fig. 11(b), the electric field strength is high, the material removal rate is high, and the original strip texture is processed. Because of the non-uniformity of the flow field and stray corrosion, the surface quality is not high, so the polishing voltage should be selected in the range of 6–8 V. The current and voltage in the ECP process exhibit a typical relationship, and four zones are formed with increasing voltage: an active zone, a passive zone, a transient zone, and a transpassive zone [25,26,27]. A large amount of passive film is produced in the passive zone, which helps in reducing the stray corrosion and improving the polishing effect of ECMP. Habibzadeh et al. found that a high voltage (ranging from 2.5 V to 10 V) decreases the grain boundary grooves. However, the surface roughness did not improve. In fact, hemispherical pits appeared when the electropolishing voltage was 10 V [30].

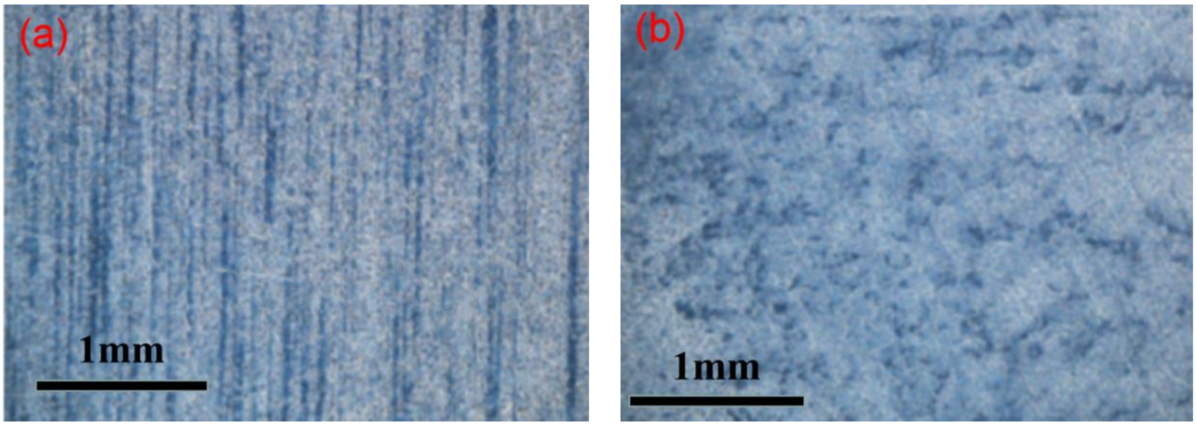

Figure 11. Microsurfaces under different voltages: (a) 4 V (Ra 0.35 μm);(b) 10 V (Ra 0.392 μm)

4.4 Duty cycle

A pulsed DC current provides a better surface quality than a continuous DC in electrochemical polishing. The duty cycle represents the ratio of the positive pulse time to the pulse period in a single pulse cycle [28]. During the processing, the ions around the cathode are consumed, and a concentration difference is produced between the cathode and the electrolyte. At the interval of the pulse, the ions around the cathode are supplemented by the diffusion of the electrolyte, and the electrolytic products and the heat are taken away to ensure the continuous renewal of the electrolyte. Figure 12 shows the relationship between the surface roughness and the duty cycle of the workpiece.

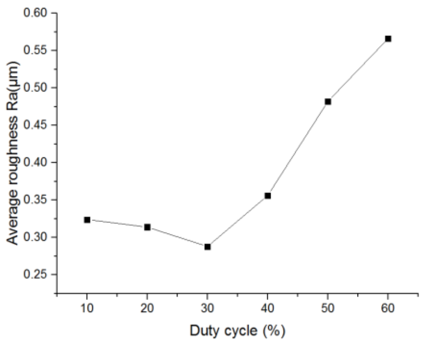

Figure 12. Influence of duty ratio on the surface roughness.

When the duty cycle reaches 40%, the surface roughness of the workpiece is high. With the increase in the duty cycle, the pulse width of the pulse power supply increases, and the electrochemical products and heat cannot be discharged in time. On the contrary, when the duty cycle is low, the electrolyte is updated timely, and an ideal surface roughness can be obtained. When the duty cycle is 30%, the microsurface of the workpiece is shown in Fig. 13. Kim and Park reported an optimum pulse time of 0.8 ms for improving the corrosion resistance of stainless steel 316L specimens when using an NaCl solution as the electrolyte [29]. Therefore, the selected duty cycle range was set in the range of 20–30%.

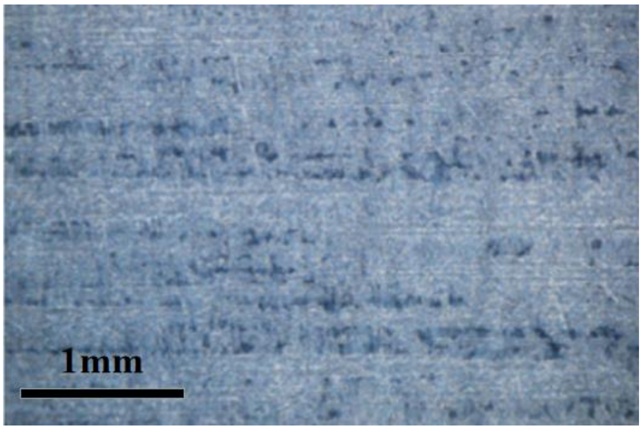

Figure 13. Microsurface of the workpiece processed under a duty cycle of 30% (Ra: 0.288 μm)

4.5 Rotational speed

In NC ECMP, the high-speed rotating composite cathode has two main functions: On the one hand, the passivation film produced by the electrochemical action on the workpiece surface is removed timely by mechanical grinding, and the electrolytic corrosion products are discharged into the electrolyte circulation filtration system under the effect of electrolyte scouring, thus ensuring a uniform conductivity in the processing area. On the other hand, the rotating speed of the composite cathode affects the efficiency of mechanical grinding, and appropriately setting the rotating speed can help improve the working efficiency while ensuring the machining quality. Under the same test conditions, the roughness of the workpiece surface is Ra 0.892 μm when the cathode speed is 500 rpm. The roughness values at rotating speeds of 1000 rpm and 1500 rpm are Ra 0.665 μm and Ra 0.462 μm, respectively, and the roughness values at cathode speeds of 2000 rpm and 2500 rpm are Ra 0.446 μm and Ra 0.435 μm, respectively. The surface roughness of the workpiece first decreases with the increase in the cathode speed, eventually reaching a minimum at a rotating speed of 1500 rpm. With the increase in the spindle speed to 2500 rpm, the surface roughness value changes little. This is because when the cathode rotation speed is low, the polishing plate cannot remove the passivation film evenly in time, resulting in an unevenly exposed workpiece surface. Therefore, the exposed surface continues to be removed by the electrolytic reaction, and the covered surface is protected without participating in the electrolytic reaction, resulting in an uneven surface of the workpiece, and therefore higher roughness. When the rotating speed of the cathode exceeds 1500 rpm, the passivation film can be removed timely and evenly. Because of the efficiency of the electrolytic polishing, the roughness obtained by polishing does not change significantly with the increase in the cathode speed. Figure 14 shows the microsurface of the workpiece when the rotating speed is 1500 rpm. Pa studied the effect of the rotational speed of a tool on the ECMP performance by varying the rotational speed from 200 to 1200 RPM. The author reported that a high rotational speed of the polishing tool can have a better effect on grinding and electrochemical finishing [19,31]. However, a high rotational speed will shorten the life of the polished plate, so the cathode speed range was set in the range of 1500–2000 rpm.

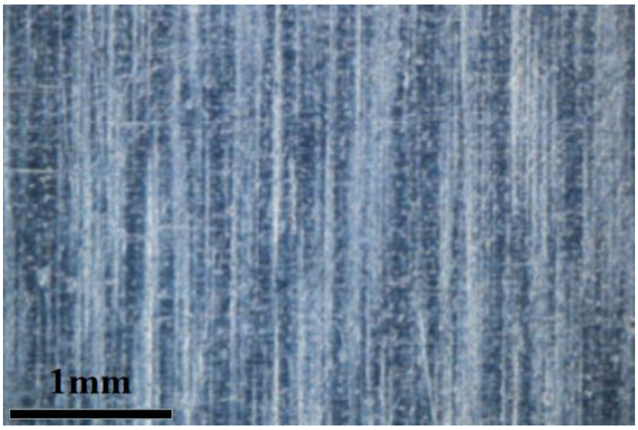

Figure 14. Microscopic surface at a cathode speed of 1500 rpm (Ra: 0.462 μm)

4.6 Feeding rate

When the polishing area is fixed, the cathode feed rate directly determines the polishing time and efficiency. When the feed rate is low, the working time of the cathode in unit length is long, the action times of the electrolytic polishing and mechanical grinding are high, and the micro high points on the workpiece surface are effectively removed, thus obtaining a better surface quality. However, when the feed speed is low, the polishing time of the integral impeller will be longer, and the efficiency will be reduced. Therefore, it is particularly important to study the polishing quality under different feed rates. In the experiment, the machining voltage is 8 V, the duty cycle is 20%, and the cathode speed is 1500 rpm. Figure 15 shows the relationship between the workpiece surface roughness and the cathode feed speed. When the feed rate increases from 10 mm/min to 70 mm/min, the surface roughness changes significantly. This is because when the feed rate is low, the polishing plate can effectively remove the passivation film on the micro high points of the workpiece surface, so as to obtain a better surface quality. When the feed speed exceeds 80 mm/min, the increase rate of the roughness value becomes lower, and the polishing time per unit area becomes shorter at higher speeds. The working time of mechanical grinding is short, and the surface quality is decreased. Figure 16 shows the microsurface of the workpiece when the feed rate is 40 mm/min. The surface texture is evenly distributed, and the quality is good. An appropriate feed rate should be selected depending on the final requirements for the polishing of blisks. To improve the surface quality and efficiency, a higher feed rate and multiple machining can be adopted. In their paper on electrochemical surface grinding using a multi-objective programming method, Ilhan et al. reported a significantly higher electrochemical action and lower mechanical forces at high feed rates of the cathode; however, the surface roughness was poor. A high feed rate is associated with higher polishing forces, faster polishing, higher total metal removal rates, and higher Ra value [32].

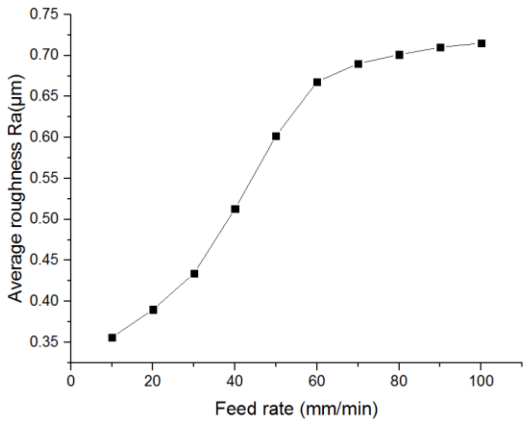

Figure 15. Influence of feed rate on the average roughness.

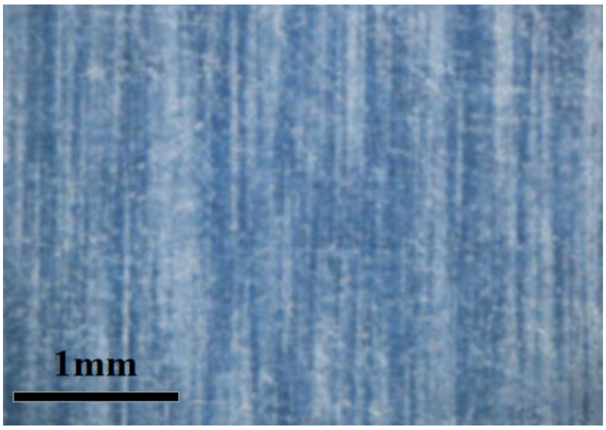

Figure 16. Microscopic surface at a feed rate of 40 mm/min (Ra: 0.526 μm)

4.7 NC row spacing

The row spacing is an important parameter in NC ECMP. It is the distance between two adjacent tool paths, which depends on the cathode diameter and the quality requirements of the polished surface. The size of the row spacing also affects the surface roughness and polishing efficiency of the polished surface. Figure 17 shows that, when the voltage is 8 V, the duty cycle is 20%, and the rotating speed of the cathode is 1500 rpm, the roughness of the polished surface increases gradually with the increase in the line spacing. When the row spacing is small, the polishing time and times in the same area are high, and the surface quality is better. However, with the increase in the line spacing, the polishing time and times per unit area gradually decrease, and the surface quality decreases. Note that the line spacing determines the polishing efficiency; not the fact that the smaller the row spacing, the better; and it should be determined depending on the actual requirements. Kang et al. studied the factors influencing the electrochemical machining of a ball-end cathode. They found that the row spacing of the ball-end cathode and other machining parameters determine the roughness value of the workpiece surface after machining and that a smaller path distance is conducive to the surface quality [34].

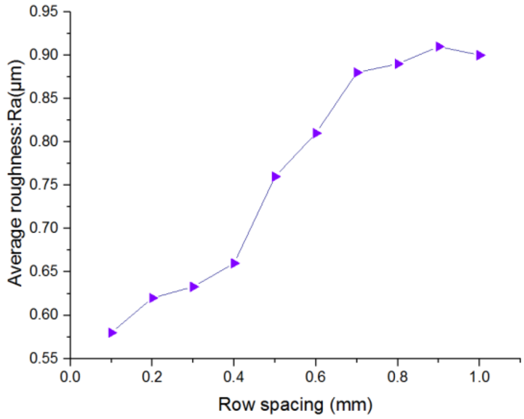

Figure 17. Influence of row spacing on the average roughness

4.8 Press force of the cathode

In theory, a higher pressure can effectively improve the removal efficiency and polishing quality of a passive film; however, a higher pressure will accelerate the wear rate of the polyurethane polishing plate and make the cathode undergo a deformation, so it is necessary to determine the appropriate pressure value. Measuring the pressure directly is inconvenient. In this study, the cutting depth is taken as the object to study the pressure indirectly, i.e., when the polishing plate is just in contact with the workpiece, the cutting depth is set to 0 mm, and the pressure is 0; when the cutting depth is 0.05 mm, the pressure value is approximately 0.01 kg/mm^2. When the cutting depth is 0.1 mm, the pressure value is approximately 0.23 kg/mm^2, the roughness is Ra 0.38 μm, and the life of the polishing piece is 3.8 h. When the cutting depth is 0.15 mm, the pressure is approximately 0.48 kg/mm^2, the roughness is Ra 0.262 μm, and the life of the polished wafer is 3.8 h. When the cutting depth is 0.2 mm, the excessive pressure leads to a significant deformation of the polishing piece, and the polishing cannot be completed. Therefore, a cutting depth of 0.1 mm is suitable for the blade disc. The press force in ECM is ten times lower than that in conventional CMP during flat polishing [33]. Lee et al. reported that a carrier table can operate even when the press pressure exceeds 1.2 kg/cm^2. The appropriate press pressure for planarization is 1.0 kg/cm^2 [16,19].

4.9 Five-axis NC ECMP of integral impeller

The five-axis NC ECMP of an integral impeller can be categorized as a finishing process. The objective is to improve the surface quality of the impeller. After mechanical cutting, the surface of the impeller will have evident strip convex blade marks, and the surface roughness value is high, approximately Ra 0.85 μm. Through the above basic tests, it is found that a high-quality polishing cannot be achieved by one-time tool feeding, and a multiple polishing technique with variable parameters is required to improve the surface roughness of the impeller. The five-axis CNC polishing program should be compiled in the test. First, the post-processing file is customized on the basis of the structural parameters of the machine tool, as shown in Fig. 2. Subsequently, the program is compiled through the NC machining automatic programming software. The following parameters should be considered in the program formulation: the cathode size, impeller hub size, blade root angle, and control of the angle between the cutter shaft and the blade to ensure that the cathode bare edge is directly opposite to the blade. Figure 18(a) shows the polishing path of the tool. The tool cathode polishing edge is laid along the single-layer spiral of the blade profile screw. The trajectory spacing is an important polishing parameter. In multiple polishing, the setting value can be in the order from high to low, which can improve the polishing efficiency and surface quality. In this experiment, a single blade was polished in three steps to reduce the Ra value. Table 2 lists the polishing conditions and results of each time. Figure 18(b) shows the clamping and polishing processes of the impeller. The cathode diameter is φ 6 mm, and the diameter of the polishing plate is φ 7 mm.

Table 2. Parameters and results of polishing

	Voltage (V)	Feed rate (mm/min)	Path distance (mm)	Rotational speed (rpm)	Duty cycle (%)	Cuttin g depth (mm)	Polishing gap (mm)	Polishin g current (A)	Ra (μm)
Step 1	9	70	0.5	2000	40	0.05	0.45	3.5	0.446
Step 2	8	50	0.3	1500	35	0.1	0.4	2.8	0.302
Step 3	6	30	0.1	1500	30	0.1	0.4	2.4	0.215

To eliminate the evident strip-shaped cutting marks left by the impeller after mechanical cutting, the parameters of the ECMP are gradually reduced from the first step to the third step. This is because the first step should efficiently reduce the Ra value and the height of the micro-convex parts on the impeller surface. Although the total polishing time in this step is short, the convex stripes cannot be completely eliminated. Sometimes, to obtain a better Ra value, the polishing parameters need to be gradually reduced. In the second and third steps, the polishing parameters lead to a low efficiency and long polishing time; nevertheless, the surface quality is good. To avoid interference in five-axis polishing, the angle of the cathode axis is adjusted by the polishing program. In other words, during the polishing process, the speed of the cathode with an equal arc length is not uniform. Sometimes, the ball head of the cathode polishing will get stuck on the workpiece surface, and the cutter shaft may swing, which increases the local polishing time, increases stray corrosion, and makes the Ra value of the blade surface inconsistent; this is a problem that should be studied further. It takes approximately 3.2 h to polish a blade in three steps. The quality of the blade surface is evidently improved (however, the polishing effect is not uniform). The best surface roughness of the blade edge is Ra 0.215 μm, as shown in Fig. 19.

Many studies have been conducted on blade polishing. He et al. designed a series-parallel hybrid platform using an abrasive belt as the tool and integrated the measuring equipment to achieve an in-situ measurement of blade polishing. However, the degree of machining allowance subdivision was determined by the conventional polishing process, which should be further optimized [36]. Wenbo et al. conducted an orthogonal central combination test on a five-axis CNC machine comprising X, Y, Z, and A axes (swing axes of the flexible grinding head) and a C axis (swing axis of the blade), with an abrasive cloth wheel as the polishing tool. The results showed a significant linear correlation between the blade surface roughness values before and after polishing [37]. The "five-axis numerical control + flexible grinding head + elastic grinding tool" polishing process was confirmed to have advantages such as high precision, little interference, and good adaptivity [38]. To improve the surface roughness and reduce the residual stress of a Ti–6Al–4V blade, Zhen et al. carried out a sensitivity analysis on the influence of polishing process parameters, proposed an optimization method for the process parameter intervals, and obtained comprehensive optimal intervals [39]. In summary, the NC ECMP has evident advantages in terms of the surface stress, tool life, and polished surface quality.

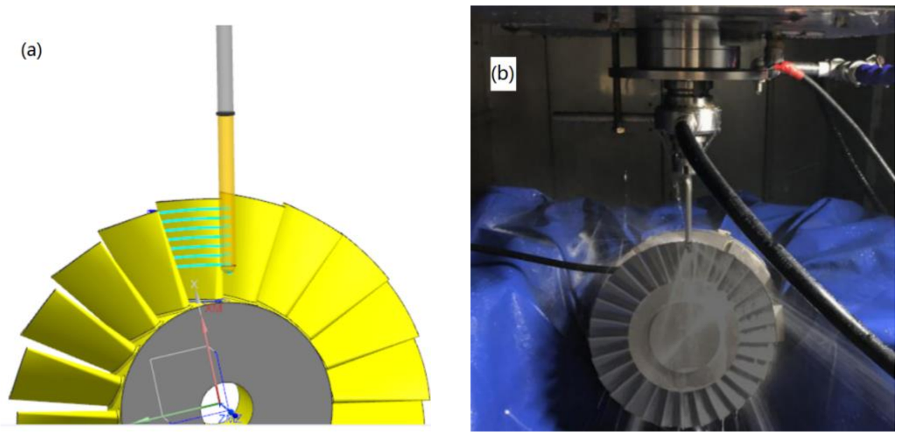

Figure 18. ECMP an integral impeller: (a) Polishing track, (b) polishing process.

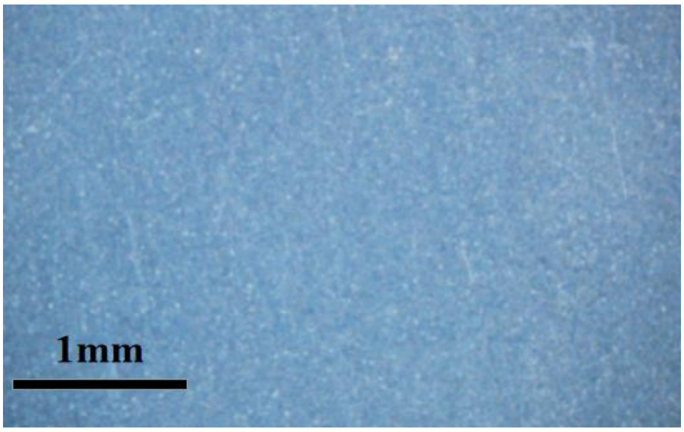

Figure 19. Best roughness of the blade edge is Ra 0.215 μm

5. CONCLUSIONS

The following conclusions can be drawn from the experimental results.

1. Under the same test parameters, a better Ra value could be obtained when using a polyurethane polishing chip instead of a CBN polishing chip. This is because the workpiece surface in the case of CBN composite cathode polishing showed evident mechanical wear marks, whereas polyurethane could effectively remove the passive film and did not cause any secondary damage to the workpiece surface.

2. The electrolyte formulation suitable for YG8 cemented carbide polishing was studied by conducting an orthogonal test. The mass fractions of the components, namely $NaNO_3$, NaOH, EDTA, and EG, were 6%, 10%, 10%, and 4%, respectively.

3. Considering the polishing efficiency and stray corrosion, the suitable polishing voltage for YG8 should be in the range of 6–8 V, and the duty cycle should be in the range of 20%–30%.

4. Increasing the rotational speed helped improve the surface roughness; however, the Ra value was less affected by the rotational speed beyond a certain speed.

5. When the feed speed was low, the Ra value increased gradually with the increase in the feed speed. Too high a feed rate was unsuitable for NC ECMP.

6. When the row space was small, although the Ra value was lower, the polishing efficiency was low. When the distance was large, the Ra value and polishing efficiency increased.

7. Although a positive pressure improved the surface roughness, the wear of the polished wafer was accelerated.

8. The optimized parameters were applied to the five-axis NC ECMP of an integral impeller. The experimental results showed that the surface roughness and efficiency could be improved by multiple polishing with variable parameters.

ACKNOWLEDGMENTS

The financial aids of the National Natural Science Foundation of China under grant NO.51705040 and Provincial Key Research and Development Projects Foundation of Jiangsu Province (BE2018), Natural Science of Foundation of the Jiangsu Higher Education Institutions of China (Granted NO.19KJA430005) are gratefully acknowledged.

References

1. I.F. Zidane, K.M. Saqr, G. Swadener, X. Ma, M.F. Shehadeh, *Int. J. Energy Res*., 40(2016)2054.
2. L. Priegue, T. Stoesser, *Int. J. Mar. Energy*, 17(2017)136.
3. J.P. Bons, *J. Turbomach.*, 132(2010)1004.
4. Y.W. Liu, H. Yan, L. Fang, L.P. Lu, Q.S. Li, L. Shao, *J. Sci China Tech Sci*., 59(2016)795.
5. T. Bai, J. Liu, W. Zhang, Z. Zou, *J. Propulsion Power Res*., 3(2014)82.
6. M.W. Pinson, T. Wang, *J. Turbomach.*, 122(2000)301.
7. M.W. Pinson, *J. Turbomach*., 122(2000)308.
8. D.A. Axinte, J. Kwong, M.C. Kong, *J. Mater. Process. Technol*., 209(2009)1843.

9. J. Wang, D. Zhang, B. Wu, M. Lou, Y. Zhang, *Int. J. Adv. Manuf. Technol*., 19(2015)405.
10. H. Huang, Z. M. Gong, X.Q. Chen, L. Zhou, *J. Mater. Process. Technol*., 127(2002)140.
11. T.R. Loveless, R.E. Williams, K.P. Rajurkar, *J. Mater. Process. Technol*., 47(1994)133.
12. R.E. Williams, V.L. Melton, *J. Rapid Prototyping*, 4(1998)56.
13. A.F. Tehrani, J. Atkinson, *Proc. Instn. Mech. Engrs*., 214(2000)259.
14. J. Kozak, K.P. Rajurkar, Y. Makkar, *J. Mater. Process. Technol*., 149(2015)426.
15. J.J. Sun, E.J. Taylor, R. Srinivasan, *J. Mater. Process. Technol*., 108(2001)356.
16. S.J. Lee,Y.H. Chen, C.P. Liu, T.J. Fan, *Int. J. Electrochem. Sci*., 8(2013)6878.
17. V.M. Volgin, T.B. Kabanova, A.D. Davydov, *Chem. Eng. Sci*., (2018)
18. W. Konstantin, W. Martin, J. Anne, W. Olivier, N. Harald, *J. Adv. Manuf. Tec*., 82(2016)197.
19. Mohammad, A.E. Khalick, D. Wang, *Int. J. Adv. Manuf. Technol*., 86(2016)1.
20. N. Kulyk, C.Y. An, J.H. Oh, S.M. Cho, C. Ryu, Y.K. Ko, C.H. Chung, Korean *J. Chem. Eng*., 27(2010)310.
21. S. Jeong, J. Bae, H. Lee, Y. Lee, B. Park, H. Kim, S. Kim, H. Jeong, *Sens. Actuators*, A, 163(2010)433.
22. H. Ramasawmy, L. Blunt, *Int. J. Mach. Tools Manuf*., 42(2002)567.
23. S. Aksu, F. M. Doyle, *J. Electrochem. Soc*., 149(2002)352.
24. J. Huo, R. Solanki, J. Mcandrew, *J. Mater. Eng. Perform*, 13(2004)413.
25. J. Lee, J. Lai, *J. Mater. Process Tec*., 140(2003)206.
26. T. Lin, C. Su, *Int. J. Adv. Manuf. Techonl*., 36(2008)715.
27. P. Tailor, A. Agrawal, S. Joshi, *Int. J. Mach. Tools Manuf*. 66(2013)15.
28. C. Sulyma, P. Goonetilleke, D. Roy, *J. mater. Process. Technol*., 209(2009)1189.
29. Y. Kim, J. Park, *Trans. Nonferrous Metals. Soc. China*, 22(2012)876.
30. S. Habibzadeh, L. Li, D.T. Shum, E.C. Davis, S. Omanovic, *Corrosion ence*., 87(2014)89.
31. PA, S. Pai, *J. Adv. Mech. Des. Syst. Manuf*., 2(2008)587.
32. R.E. Ilhan, G. Sathyanarayanan, R.H. Storer, T.W. Liao, *Int. J. Mach. Tools Manuf*., 32(1992)435.
33. D. Lee, H.J. Kim, B.J. Pak, D. Kim, H. Jeong, H. Lee, *J. Frict. Wear*, 38(2017)482.
34. M. Kang, X.Q. Fu, Y. Yang, *Adv. Mater. Res*., 154(2010)338.
35. Y.F. He, J.S. Zhao, H.X. Xiao, W.Z. Lu, W.W. Gan, *Int. J. Electrochem. Sci*., 13(2018)5736.
36. Q. He, J. Zhao, M. Feng, C. Zhang, H. Chen, *Int. J. Adv. Manuf. Technol*., 102(2019)265.
37. W.B. Huai, H. Tang, Y.Y. Shi, X.J. Lin, *Int. J. Adv. Manuf. Technol*., (2017).
38. W. Huai, Y. Shi, H. Tang, X. Lin, *J. Mech. Sci. Technol*., (2019).
39. Z. Chen, Y.Y. Shi, X.J. Lin, T. Yu, P. Zhao, C. Kang, X.D. He, H.L. Li, *Results Phys*., 12(2019)870.